

Shi, Z. and Chen, Q. 2021. "Experimental and computational investigation of wall-mounted displacement induction ventilation system," *Energy and Buildings*, 241: 110937.

Experimental and Computational Investigation of Wall-mounted Displacement Induction Ventilation System

Zhu Shi, Qingyan Chen*

School of Mechanical Engineering, Purdue University, West Lafayette, IN 47907, USA

*Phone: (765) 496-7562, Fax: (765) 496-0539, Email: yanchen@purdue.edu

Abstract

Traditional displacement ventilation (DV) creates high indoor air quality in occupied zone in cooling season due to thermal plume created by heat sources which then effectively purge contaminants out of the breathing zone, but tend to be challenged when high cooling loads are present. In addition, traditional DV, when supplying heated air via its diffusers has low ventilation effectiveness in heating season. This study investigated a novel wall-mounted displacement induction ventilation (DIV) system in comparison to traditional DV system. The investigation used an environmental chamber to mimic a typical classroom and measured the distributions of air velocity, air temperature, and contaminant concentration for validating the subsequent computational fluid dynamics (CFD) model developed across an array of operational modes. Then the CFD model was employed to evaluate the performance of DIV system in terms of ventilation effectiveness, mean age of air and vertical temperature gradient as it relates to thermal comfort. Each DIV unit receives 100% outdoor (or primary) air to its plenum chamber. As the primary air pressurizes the chamber, it exits a series of nozzles, creating a low pressure which then induces room air across the integral hydronic coil. A room is typically supplied with multiple DIV units, which allows for individual control operation during both cooling and heating modes. Results showed that stratified air distribution was achieved in both cooling and heating modes with DIV system, which remedied the current limitation of traditional DV.

Key words:

Displacement ventilation, Ventilation effectiveness, Thermal comfort, Age of air, Classroom

Nomenclature

C	Contaminant concentration	T_e	Air temperature at exhaust
$C_{1.1m}$	Contaminant concentration at head level of a seated person	$T_{1.1m}$	Air temperature at head level of a seated occupant
C_e	Contaminant concentration at exhaust	$T_{0.1m}$	Air temperature at ankle level
C_o	Outdoor contaminant concentration	T^*	Normalized temperature
C_p	Specific heat at constant pressure	u_i	Velocity in direction i
C^*	Normalized contaminant concentration	U	Velocity magnitude
E	Energy per unit mass	U^*	Normalized velocity
F	Force	VE	Ventilation effectiveness
g	Gravitational acceleration	x_i	Coordinate in direction i

h	Height	$\Gamma_{\phi,eff}$	Turbulent diffusion coefficient of scalar ϕ
H	Height of room	ΔT_{ha}	Temperature difference between head and ankle levels
H^*	Normalized height	ε	Turbulent dissipation
k	Turbulent kinetic energy	ν	Kinematic viscosity
MAA	Mean age of air	ν_t	Turbulent eddy viscosity
S_ϕ	Source of scalar ϕ	ζ	Random number
T	Air temperature	ρ	Density
$T_{0.1m}$	Temperature at ankle level	ρ_p	Density of particle
$T_{1.1m}$	Temperature at head level (seated occupant)	ϕ	Scalar
T_s	Temperature of supply air		

1. Introduction

According to the Environment Protection Agency (EPA), an average American spends around 90% of his or her lifetime indoors [1, 2]. To improve the well-being and productivity of occupants, it is needed to create satisfactory indoor environment quality (IEQ) inside buildings. Indoor air quality and thermal comfort are two essential aspects for appraising IEQ [3], and the ventilation system inside a building should be well developed to fulfill the expectations on these two aspects. Among various types of ventilation systems, traditional displacement ventilation (DV) systems, which supplies clean air to the lower part of a room and exhausts air from ceiling, provides higher indoor air quality (IAQ) than a traditional mixing ventilation (MV) system when used for cooling [4, 5, 6]. However, the IAQ benefit of traditional DV systems only exists under cooling seasons. When it is used for heating, the heated fresh air from traditional DV diffusers takes an immediate path upwards, due to buoyancy effects, into the unoccupied zone, which results in poor IAQ in occupied zone [7, 8]. Besides, in cooling seasons, since traditional DV supplies air to occupied zone directly, its supply air temperature could not be too low [9, 10], for thermal comfort reasons which greatly limits traditional DV's capability to remove high cooling loads. In fact, Cho et al. [11] and Yuan et al. [12] showed that a traditional DV system was not suggested when the cooling load was higher than 40 W/m². These limitations greatly hinder the applicability of existing traditional DV systems.

In order to expand the applicability of traditional DV systems, previous studies tried coupling traditional DV with a water system, such as chilled ceiling (CC) or passive chilled beams (PCB). For example, Rees and Haves [13] and Loveday et al. [14] showed that a coupled traditional DV-CC system could remove 62 W/m² of cooling load while still maintaining satisfactory thermal comfort. Shi et al. [15] evaluated the performance of a coupled traditional DV-PCB system and concluded that PCB was a very effective complement for reducing the vertical temperature gradient caused by traditional DV. However, since CC and PCB were installed near ceiling in these coupled systems, the cooled air could generate local downward airflow that brought airborne contaminants down to occupied zone [16, 17] unfortunately negatively impacting IAQ levels. Moreover, these coupled traditional DV-water systems are still not applicable in heating seasons: if hot water passes through CC or PCB, the air warmed by hot water coils stayed at upper part of the room rather than entering occupied zone. Therefore, further improvements were needed to continue addressing the above-mentioned limitations.

This study investigated a novel displacement induction ventilation (DIV) system for remedying these problems of traditional DV-water systems. The DIV system consists of multiple DIV units in

an array that were installed on the floor against the wall. Rather than suspending the water system near the ceiling, this system integrates heating and cooling coils into each DIV unit. When the primary (outdoor) air is supplied to the plenum and the air exits through nozzles, it entrains the room air across the integral hydronic coil. The room air is sensibly cooled or heated in response to a thermostatic setting then mixes with primary air before the newly conditioned supply air is discharged to the room. In cooling mode operation, all units were used for cooling. In heating mode operation, some units were used for heating and others still supplied air with a slightly lower temperature than room air. As an alternative heating approach, each DIV unit could also be equipped with optional rear finned tube type coils so the units could also be operated such that these finned tube coils could address heating loads while cool ventilation air is supplied to occupied zone. These unique control and equipment strategies have the capability of achieving stratified air distribution, and thus ventilation effectiveness that is greater than unity, in both cooling and heating seasons. Hence, these strategies give DIV system great potential to enhance the applicability over traditional DV system.

Therefore, this research tried to explore the ventilation and thermal performance of the novel DIV system. A DIV system was first set up in an IAQ chamber to measure the distributions of air velocity, air temperature and contaminant concentration. The experimental data was used to validate a computational fluid dynamics (CFD) model. With the validated CFD model, this study analyzed the airflow and contaminant distributions in a modeled life-size classroom with the DIV system during both cooling and heating modes in accordance with ASHRAE 62.1-2019, Normative Appendix C [18]. The performance of the DIV system was evaluated and compared with that of a traditional DV system. Finally, this study discussed impact of DIV system on indoor environment, as well as droplet dispersion in an indoor space with DIV.

2. Research Methods

Previous studies [19, 20, 21, 22] used both experimental measurements and CFD simulations to evaluate ventilation system performance. Although experimental method provides reliable information regarding airflow and contaminant concentration in an indoor space, constructing the experimental setup is very time-consuming and there is little flexibility in the geometry of investigated indoor space. CFD simulations solve for the indoor airflow information by numerically resolving the partial differential equations that govern the indoor airflow and contaminant transportation, which provides solution in a quick manner and allows modification of room geometry [23, 24]. However, the CFD models incorporate inherent approximations that may cause inaccuracy [25, 26]. Hence, it is critical that a CFD simulation model is validated by measurement data before it is used for analyzing the performance of an HVAC system [27].

The current study investigated the novel DIV system using combined experimental and CFD methods. This section first describes the concept of the DIV system as well as details of experimental setup and the developed CFD model. In addition, it specifies the cases used to study the performance of DIV system. Moreover, the key indices that were utilized for evaluating system's ventilation and thermal performance are defined.

2.1 Description of DIV unit and DIV system

Fig. 1 shows the 3D geometry of a DIV unit, in which chilled and hot water coils are installed in its upper part. Aluminum fins (not shown on the figure) are configured perpendicularly to coils to enhance heat transfer. Outdoor air is introduced to the plenum noted where an elevated plenum pressure is produced. The plenum pressure is the driving force; the plenum pressure drives the air across a series of nozzles downward inside the unit, behind the hydronic coil. As the air exits the nozzles, a resulting low-pressure area is created and correspondingly induces room air before the mixed (outside and room) air is discharged to the room (Fig. 2). Depending on the operating mode

of the unit, the induced air could be heated or cooled by the circulating hot or chilled water in response to the room thermostat setting or mode. Optional, rear finned tube heating coils are installed on the back wall behind each unit to provide an alternative heating approach, more often applied in extremely cold climate conditions, which are described below.

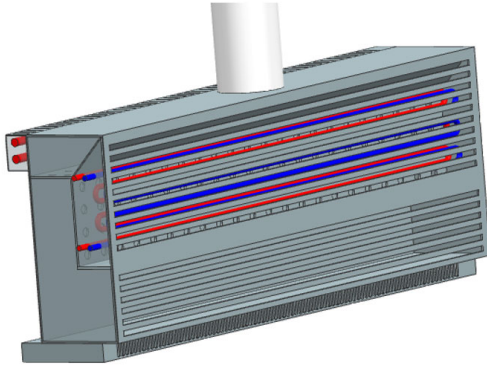


Fig. 1 3D geometry of a DIV unit

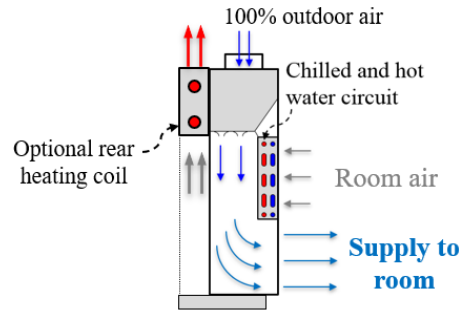
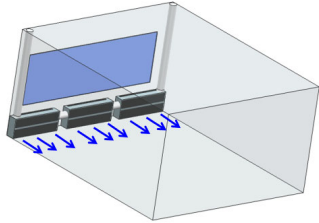
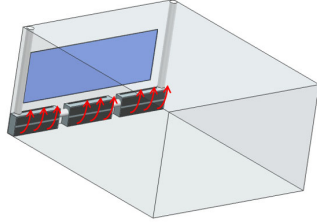
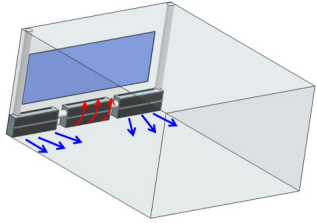
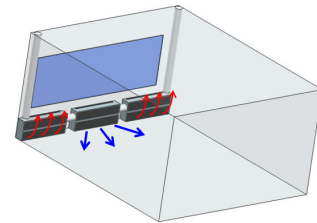
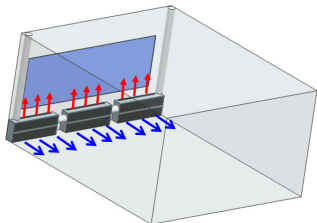


Fig. 2 Airflow patterns induced by a DIV unit

A DIV system consists of multiple DIV units. Since each unit can be thermostatically controlled individually, the DIV system can address complex thermal environments by combining the units with different operation methods, as shown in Table 1. When all units are used for cooling, the system is in “cooling mode”, as shown in Mode 1. If they are all used for heating, the system is in “full-face heating mode” (Mode 2 – Operational mode typically reserved for low occupancy times, such as morning warm up when increased input is deemed necessary). If some units are activated for heating, while others for ventilation, it is in “staged-face heating mode” (Modes 3-1 and 3-2). Lastly, the optional rear heating coils can be utilized for a specific heating methodology while cool ventilation air is supplied from the diffuser, the DIV system serves as “rear heating mode”. Compared with traditional DV system which can only create stratified air distribution in cooling season, the design of DIV system allows it to create contaminant stratification in both cooling and heating seasons through various solutions. Besides, by innovatively integrating water coils into the units, this system should also have good energy efficiency that was demonstrated in other water systems such as PCBs or ACBs. Therefore, DIV potentially combines the benefits of multiple types of systems using a single system. This research investigated the performances of the novel DIV system under different operating modes, and compared them with those in traditional DV systems.

Table 1. Different operation modes of DIV system

Mode number	Mode type	Operation mode
1	Cooling	

2	Full-face heating	
3-1	Staged-face heating I	
3-2	Staged-face heating II	
4	Rear heating	

132

133 2.2 Experimental setup

134 Airflow velocity, air temperature and contaminant concentration distributions are key pieces of
135 information for understanding the thermal and ventilation performance of an HVAC system. To
136 measure such information, this study constructed a DIV system that consists of 3 DIV units inside
137 an IAQ chamber (6.08 m × 5.15 m × 3.05 m), as illustrated in Fig. 3. Fig. 4 further shows how the
138 3 units were configured under the window in a series. In this system, conditioned outdoor air was
139 supplied to the units through two air ducts that were located at two corners, while the exhaust was
140 located on the opposite side of the chamber near ceiling which is optimal for any displacement
141 ventilation operation. Both chilled water and hot water were supplied to every unit. The chilled
142 water was from a chilled water reservoir inside the building, while the hot water was provided by
143 a water heater outside of the chamber (Fig. 4b). This experimental system could provide chilled
144 water whose temperature could be as low as 10 °C, while the temperature of hot water provided by
145 water heater could be as high as 93 °C. To minimize heat transfer between the pipes and ambient
146 air, all the exposed water pipes were well insulated.

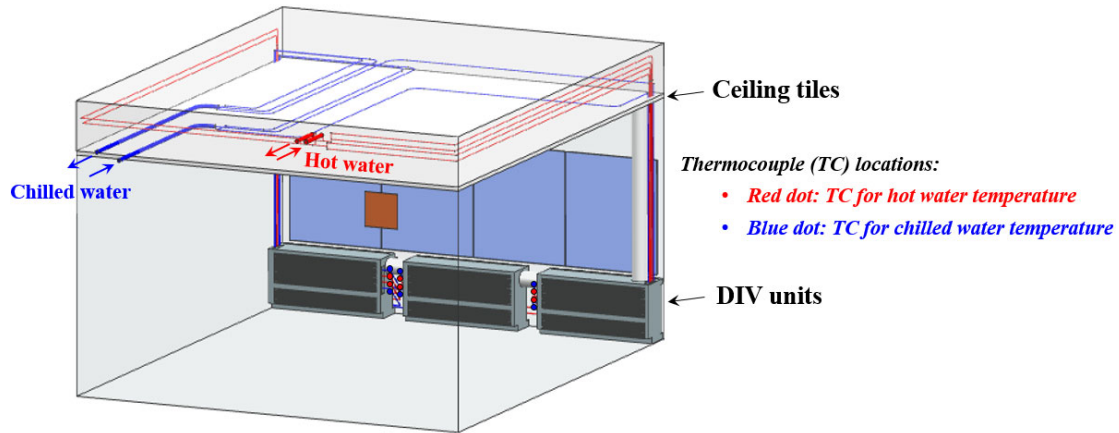
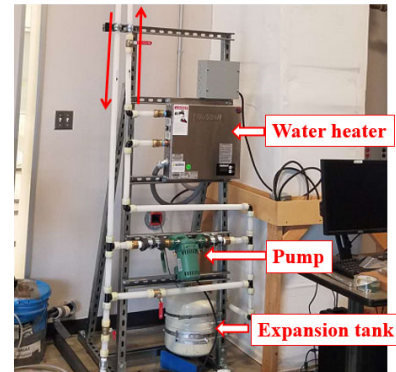


Fig. 3 Sketch of test system in IAQ chamber



(a) DIV system inside IAQ chamber



(b) Hot water supply system

Fig. 4 Photos of experimental setup

Fig. 5 shows the layout of the IAQ chamber, which included 8 human models (heated boxes) and 4 tables, to mimic a partial classroom. The dimensions and power of each human model were $0.41 \text{ m} \times 0.41 \text{ m} \times 1.13 \text{ m}$ and 84 W , respectively. Inside each dummy, light bulbs were installed to generate heat while a mini-fan was utilized to recirculate heated air, which was to uniformize the human model surface temperature. During the experiment, the supply air temperature and airflow rate were controlled by a LabView program on a computer located outside of IAQ chamber. Similarly, another LabView program was used to condition the air temperature in outdoor chamber, which simulated outdoor climate (Fig. 5). The supply water temperature of chilled water was set through the building automation system (BAS), while that of hot water was controlled on the water heater panel. Meanwhile, the water flowrate in each DIV unit could be regulated individually using valves. Besides, this study used a tracer gas, sulfur hexafluoride (SF_6), to simulate the airborne contaminant in the room. It was released from the top of a human model.

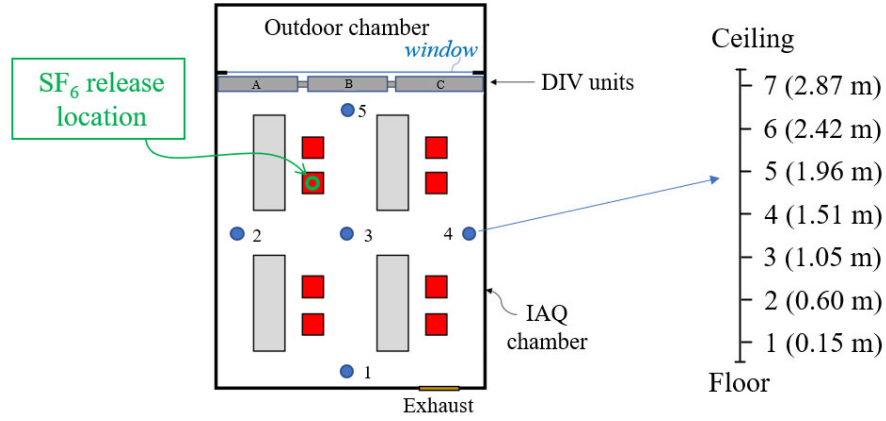


Fig. 5 Layout of IAQ chamber in experiment (Red boxes: human dummies; Blue dots: pole locations)

In the experiment, a variety of sensors were used to obtain the measurement data. Type-T thermocouples were instrumented at the inlet and outlet of water pipes in each DIV unit, as shown in Fig. 3. Meanwhile, water flow rates for every DIV unit were measured using turbine flowmeters with a measurement accuracy of $\pm 0.1\%$. Hot-sphere anemometers were utilized to measure the airflow velocity and air temperature inside the chamber. The error for airflow velocity measurement was ± 0.02 m/s, and the error for temperature measurement was ± 0.2 °C. During the test, an infrared thermometer was used to measure temperatures on heated surfaces. This study measured SF_6 concentration using a photoacoustic multi-gas analyzer [28], with corresponding measurement error being 0.01 ppm. As shown in Fig. 5, airflow velocity, air temperature and SF_6 concentration was measured on 5 different poles, with 7 evenly distributed heights along each pole. During the experiment, data acquisitions were conducted outside of IAQ chamber, so the operation of the experimental system did not affect the indoor airflow.

2.3 CFD modeling of indoor environment established by DIV system

This research developed a CFD model to investigate the airflow and contaminant distributions in indoor spaces with DIV systems. The model numerically solved Reynolds-Averaged Navier-Stokes (RANS) equations [29] by adopting Re-Normalization Group (RNG) $k - \varepsilon$ turbulence model [30, 31], which showed good performance in predicting indoor airflow characteristics [32]. The transport equations this CFD model solved could be expressed as:

$$\rho \frac{\partial \bar{\phi}}{\partial t} + \rho \bar{u}_i \frac{\partial \bar{\phi}}{\partial x_i} - \frac{\partial}{\partial x_i} \left[\Gamma_{\phi, \text{eff}} \frac{\partial \bar{\phi}}{\partial x_i} \right] = S_{\phi} \quad (1)$$

where ϕ stands for u_i , E , C , k and ε in momentum equation, energy equation, species transport equation, transport equation for k and transport equation for ε , respectively. Besides, this simulation assumed air density varied with air temperature by employing Boussinesq approximation [33, 34], which is valid since the air density variation in indoor environment was sufficiently small.

To accurately capture the airflow characteristics in the indoor space with DIV system, it is critical to prescribe appropriate boundary conditions in the CFD model. This research used non-slip temperature boundary conditions for walls and heated surfaces in the computational domain, and the corresponding temperature values were obtained from measurement. A non-buoyant point source of SF_6 was modeled to simulate the release of SF_6 . Grid independence test was performed

by examining the average airflow velocity in a $0.2\text{m} \times 0.2\text{m} \times 0.2\text{m}$ cubic volume above a human dummy, which was key for characterizing the strength of thermal plume created by a human dummy. The test was conducted under three grid numbers: 623,597 (coarse setting), 3,076,949 (medium setting) and 9,472,323 (fine setting). Comparison showed there was a difference of 27.9% between results in coarse setting and that in medium setting, and the difference between those in medium setting and fine setting was minimal. Hence, the grid number in medium setting was considered sufficient for the simulation. This study utilized ANSYS Fluent 17.1 [35] as the numerical solver for the governing equations. It employed SIMPLE (semi-implicit method for pressure-linked equations) scheme for pressure-velocity coupling and adopted second-order spatial discretization method for equation set (1). During the calculation, this research used 10^{-3} as the convergence criterion for residuals of u_i , k , ε and C , and 10^{-6} for residual of E .

2.4 Specification of cases used for performance evaluation

With a validated CFD model, this study investigated the ventilation and thermal performance of the novel DIV system under various operating modes. A typical classroom (Fig. 6) was used as the indoor space for the DIV system, and its dimensions were $9.14\text{ m} \times 9.14\text{ m} \times 2.74\text{ m}$, which was determined via NCES [36]. Three DIV units were evenly distributed against the exterior wall under the window. All the other three vertical walls were considered as interior ones. This simulated classroom contained 25 occupants (24 students and one instructor) and 6 overhead lights. The outdoor airflow rate used was 169 L/s, which was the outdoor airflow rate determined from ASHRAE Standard 62.1 -2019 [18].

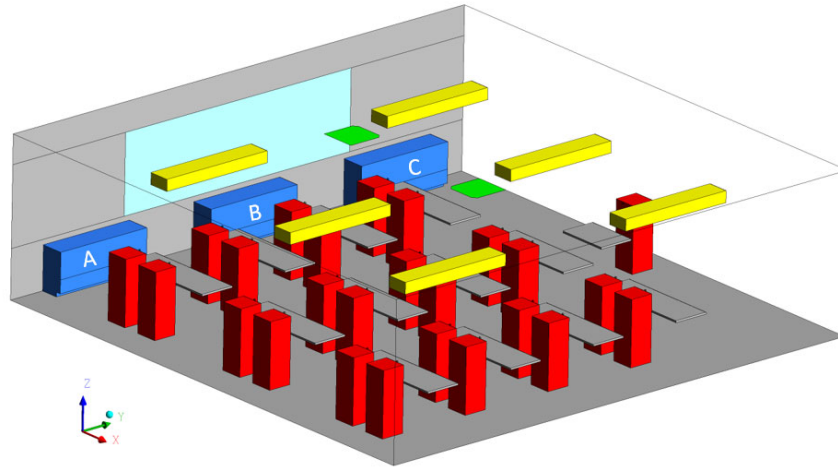


Fig. 6 Layout of a real-size classroom for studying performance of DIV system

This research explored the performance of DIV system under 4 operation modes that were described in Section 2.1. Table 2 lists the details of the studied cases. In particular, under “Staged-face heating” mode, 2 combinations of the units were studied, and their performances were compared. In addition, to compare the performance of DIV system with that of traditional DV system, this investigation also included a DV-C case and a DV-R case. Moreover, since the indoor temperature setpoints in summer and winter are normally different, this study used $23.8\text{ }^{\circ}\text{C}$ ($75\text{ }^{\circ}\text{F}$) and $22.2\text{ }^{\circ}\text{C}$ ($72\text{ }^{\circ}\text{F}$) as the setpoints in cooling cases and heating cases, respectively.

Table 2. Specifications of real-size classroom cases investigated in this study

Mode	Case #	System	Description	Outdoor airflow rate	Window interior surface temperature
------	--------	--------	-------------	----------------------	-------------------------------------

Cooling	DIV-C	DIV	3 units cooling	169 L/s	27 °C
	DV-C	DV	Traditional DV system	169 L/s	27 °C
Staged-face Heating	DIV-SH1	DIV	1 unit for heating (B) + 2 units for ventilation (AC)	169 L/s	16 °C
	DV-SH2	DV	2 unit for heating (AC) + 1 unit for ventilation (B)	169 L/s	16 °C
Full-face Heating	DIV-FH	DIV	3 units for heating	169 L/s	16 °C
Rear heating	DIV-RH	DIV	3 units for rear heating + front ventilation	169 L/s	16 °C
	DV-R	DV	Traditional DV + radiator	169 L/s	16 °C

2.5 Indices for evaluating performance of DIV system

To evaluate the ventilation and thermal performance of the novel DIV system and to compare it with that of traditional DV system, it is important to use proper indices that could quantify such performance. Hence, the following indices were employed in this study.

• Ventilation effectiveness (VE, or Ez)

This study characterized the air quality at an arbitrary location of the room as [18, 37]:

$$VE_a (or Ez-a) = \frac{C_e - C_o}{C - C_o} \quad (2)$$

where C_o , C_e and C stand for contaminant concentrations of outdoor air, at exhaust and at a selected location in a room, respectively. In particular, the average VE_a at 1.1 m above the floor is of great importance, since it describes the air quality perceived by seated occupants [37, 38]. This value was hence used as one index to assess indoor air quality and was calculated by:

$$VE(or Ez) = \frac{C_e - C_o}{C_{1.1m} - C_o} \quad (3)$$

If the room air is mixed perfectly by a ventilation system, VE is equal to 1.

• Mean age of air (MAA)

This research also adopted MAA, which characterizes the time needed for air to move from inlet to a certain location in the indoor space [39, 40, 41], to quantify the indoor air quality. It gauges the freshness level of indoor air directly. This study developed a user-defined function (UDF) in ANSYS Fluent 17.1 to solve for MAA. The transport equation of MAA could be expressed by Eq. (1) with the corresponding effective diffusion coefficient being $\Gamma_{\tau,eff} = \rho\nu + \nu_t/0.7$.

• Temperature gradient between head and ankle: ΔT_{ha}

Air temperature difference between head and ankle could lead to thermal discomfort to an occupant [42, 43]. Hence, this study used ΔT_{ha} to quantify the thermal comfort in the room:

$$\Delta T_{ha} = T_{1.1m} - T_{0.1m} \quad (4)$$

where $T_{1.1m}$ and $T_{0.1m}$ stand for air temperature at head and ankle levels of a seated occupant, respectively. For optimal thermal comfort, it is recommended that ΔT_{ha} to be less than 3 °C [44].

3. Results

In this research, experimental data was obtained to validate the developed CFD model, which was then used for system performance assessment. This section details the validation of CFD model by comparing the CFD simulation results with measured data. It then evaluated the ventilation and thermal performance of DIV system in terms of VE, MAA and ΔT_{ha} .

3.1 Model validation

This paper employed one representative case (cooling mode, 102 L/s of outdoor air) in the IAQ chamber for the validation. This case included 8 human models and 4 tables as illustrated in Fig. 5. It also had 4 overhead lamps, each with power of 64 W. The outdoor climate chamber was operated to create a summer outdoor condition and the window interior surface temperature was 27 °C. During the experiment, the SF₆ mix (1% SF₆ with 99% Nitrogen) was used as a tracer gas to simulate the airborne contaminant, and the background SF₆ concentration in atmosphere is zero. All other details regarding the case layout could be found in Section 2.2.

Fig. 7 shows the airflow velocity, air temperature and SF₆ concentration distributions on three poles (1, 3 and 5) that were on the central vertical plane of the chamber. On these plots, height, velocity, temperature and SF₆ concentration were normalized as: $H^* = h/H$, $U^* = U/U_0$ (where $U_0 = 0.2 \text{ m/s}$), $T^* = (T - T_s)/(T_e - T_s)$ and $C^* = (C - C_s)/(C_e - C_s)$. Results showed that airflow velocity was generally larger near floor than in upper region of the room, which was because air was supplied near floor. Since some room air was recirculated back into DIV units, a second peak existed on some velocity profiles, especially if the pole was close to DIV unit, such as Pole 5. Meanwhile, because of thermal plumes, a clear vertical temperature gradient could be found on the temperature profiles from both experimental and simulation data. Since air temperature distribution was mainly determined by buoyancy force that was generated by thermal plume, the temperature generally did not vary much with distance from units. In locations that are very close to units (e.g. Pole 5), the air temperature at lower part was slightly lower than that in other locations, as observed in Fig. 7. SF₆ distribution also showed a clear stratified pattern, which indicated that SF₆ concentration was generally lower in the breathing zone. Due to limit of space in this paper, comparison of results from only three poles was presented, but the results on the other two poles (2 and 4) were predicted by CFD model at similar accuracy. The discrepancies between simulation and measured results could be partially explained by the approximations in the numerical modeling process. Previous indoor environment simulations [37, 45] also showed some level of differences between simulated and measured results. For example, Chen et al. [45] reported relative discrepancies of 45%, 31% and 44% in airflow velocity, air temperature and SF₆ distributions, respectively. In current study, the overall trends of airflow and contaminant concentration distributions matched reasonably well and the discrepancy was smaller than what was reported in Chen et al. [45]. The CFD model was thus used for further assessment of DIV performance.

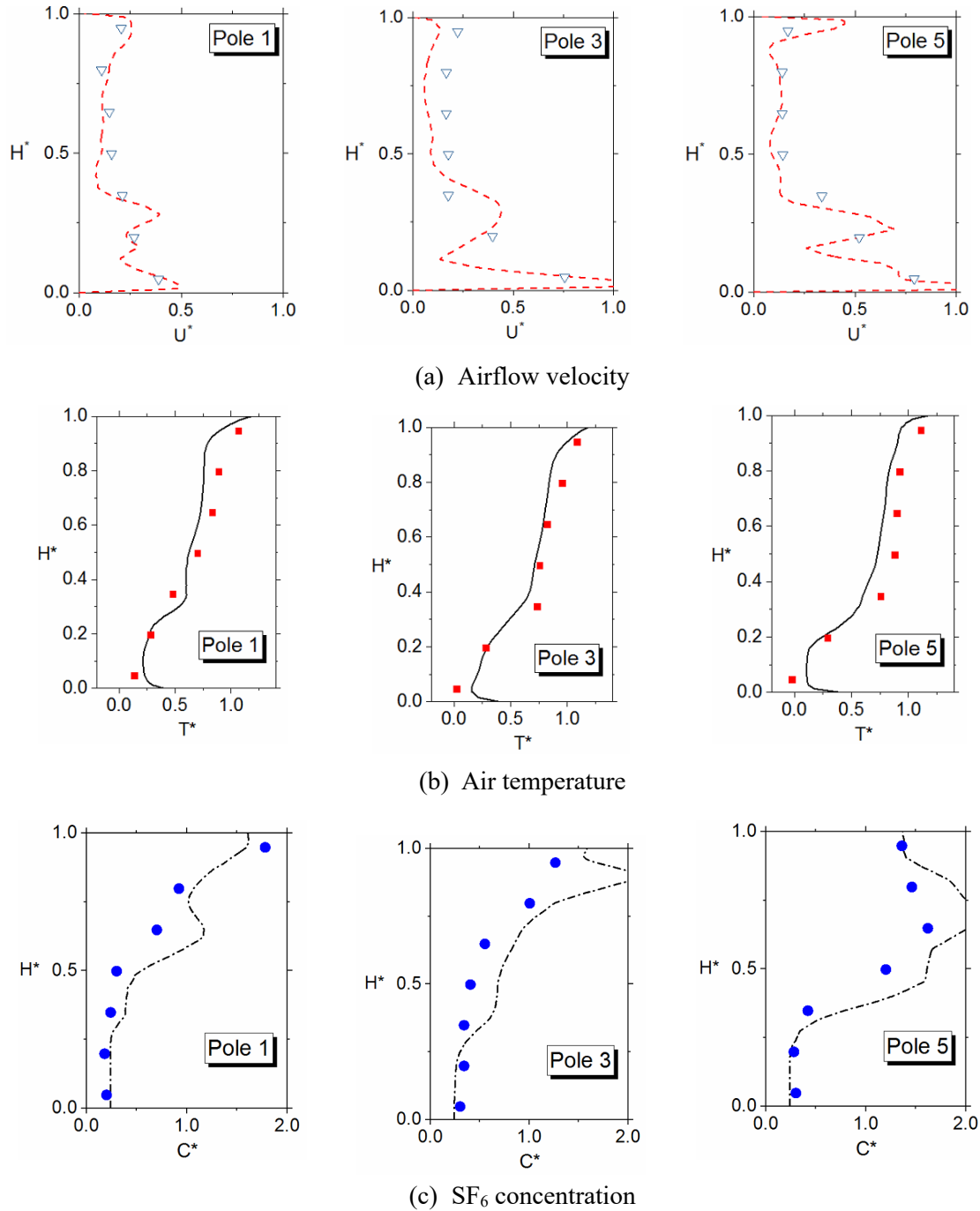


Fig. 7 Comparison of simulated and measured results in IAQ chamber (Symbols: measurement results; Lines: simulation results)

3.2 Performance in cooling mode

The validated CFD model was employed to study the indoor environment in a classroom under different cooling and heating DIV modes. Fig. 8 illustrates the airflow distributions on two representative planes in the classroom in DIV-C case. The discharged cool air flowed along the floor with a minimum exit momentum sufficient and delivered fresh air to all occupants in the classroom (Fig. 8a). Meanwhile, some air in lower part of the room was recirculated into the DIV

units as shown on the vertical cross-section (Fig. 8b). By inducing the room air low within the breathing zone, the recirculated (or induced) air is fresher than exhaust air, due to the displacement thermal plumes driving the contaminants toward the elevated ceiling heights. This airflow pattern, created by DIV displacement operation, is the critical approach for recognizing lower contaminant levels in the breathing zone, or seated areas, thusly delivering higher IAQ for occupants.

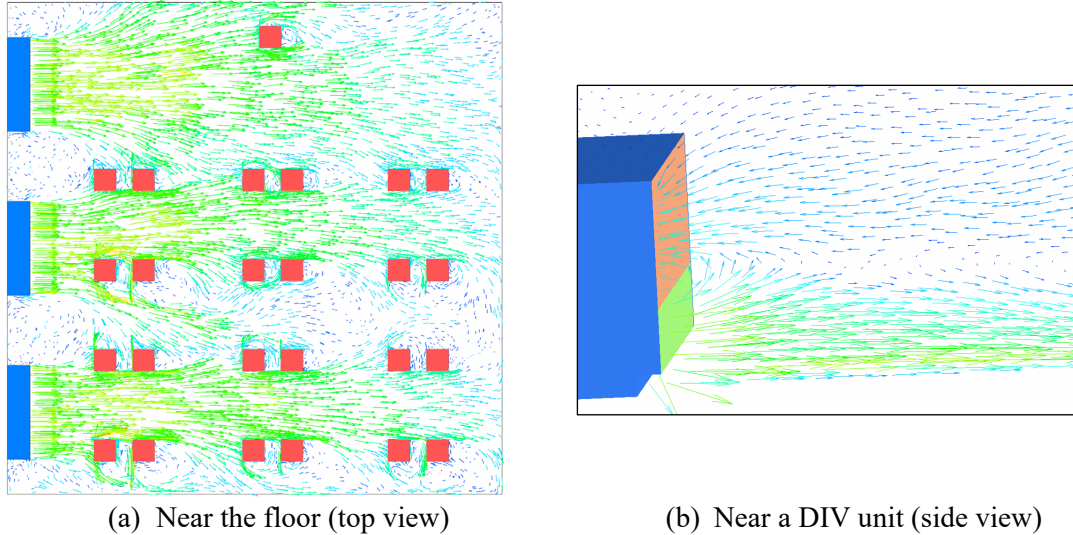


Fig. 8 Airflow distributions of two cross-sections in DIV-C case

Fig. 9(a) further showed the indoor air quality (characterized by VE_a) distribution on a representative vertical plane in DIV-C case. In the simulation, airborne contaminant was released from each of the 25 occupants at an equal rate. It can be seen from the figure that airborne contaminant moves up with thermal plumes that were generated by the occupants. Since the induced air was from lower occupied zone, its air quality was much higher than that in upper part (above the occupied zone) of the room. As a result, a clear contaminant stratification was observed and VE_a values in occupied zone were high. This is critical for predominantly seated occupants within the occupied zone, where the highest levels of fresh air are required to ensure healthy breathing environments. For comparison, Fig. 9(c) illustrated the VE_a distribution on a vertical plane in a corresponding traditional DV case (DV-C). In this traditional DV case, a large portion of the return air (corresponding to the induced airflow rate in DIV-C case) was recirculated. Referring to Figure 8 (a) and (c), it is noted VE_a in the critical seated area for DIV-C ranges between 2.2 and 1.3 as compared to DV-C where the VE_a stays between 1.3 to 1.0. The much-improved VE in the seated area of the DIV-C system is a result of the induced air in DIV-C being cleaner as compared to a similarly operated traditional DV-C. The average room VEs in DIV-C and traditional DV-C cases were 1.29 and 1.2, respectively. The drastic IAQ improvements were noted in the localized room regions where the occupants are. Meanwhile, Fig. 9(b) and Fig. 9(d) illustrated the stratified air temperature distributions in both DIV-C and DV-C. The quantitative comparison in Fig. 9(f) also showed that the temperature distributions on a vertical plane in both cases were similarly stratified. Both of their vertical temperature gradients in occupied zone met ASHRAE-55 requirement (3 °C).



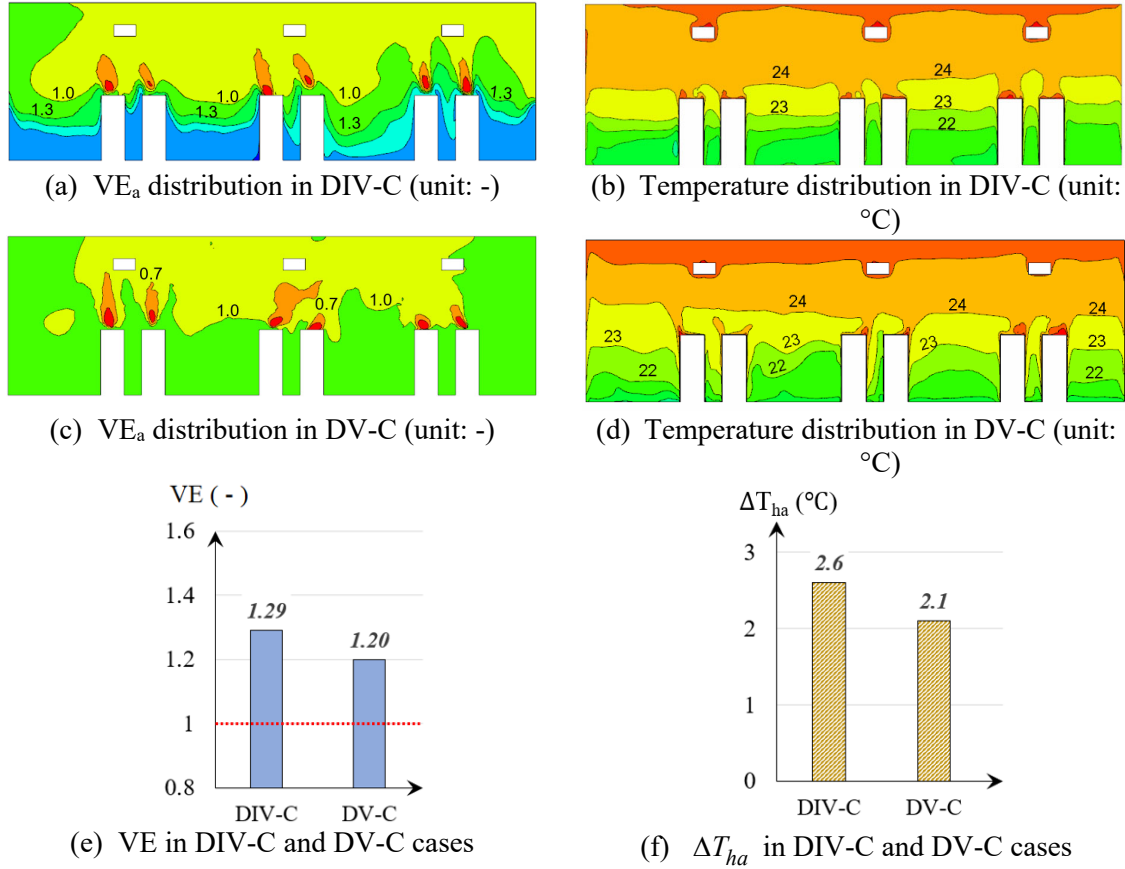


Fig. 9 Comparison between indoor environments created by DIV-C and DV-C

3.3 Performance in face heating mode

DIV system presents the ability to heat while operating in displacement due to heating mode control strategies of using one or more of the DIV units for heating. Since there are three DIV units in the investigated DIV system, three face heating options are available: two “staged-face heating” options (cases DIV-SH1 and DIV-SH2) and one “full-face heating” option (case DIV-FH). Fig. 10 illustrates the airflow distributions in a representative “staged-face heating” case. In DIV-SH1 case, unit B was on for supply of warm air (i.e. hot water active in hydronic coil) to the space while units A and C were in ventilation mode with no added heat from their respective hydronic coil. Warm air discharged from unit B went slowly out into the room, while horizontal travel of supply air was aided by the ventilation air (no heat on) discharged from units A and C. This combination of ventilation and warm air was then further heated up by the heat sources in the occupied zone and moved up into the unoccupied zone. As was recognized in the cooling mode, a large portion of clean air reaches the breathing zone under this combined operating strategy. Note that although the air discharged by units A and C was considered “cool” as compared to the air temperature in the bulk region of the room, the cool ventilation air temperature was elevated relative to outdoor air in heating season for occupant thermal comfort. Therefore, this unique control strategy of supplying a combination of warm and “cooler” ventilation air to the room simultaneously (some units delivering the ventilation air while the remainder delivering warmer air) produce stratified room conditions, maintain occupant thermal comfort levels, and does not waste additional energy.

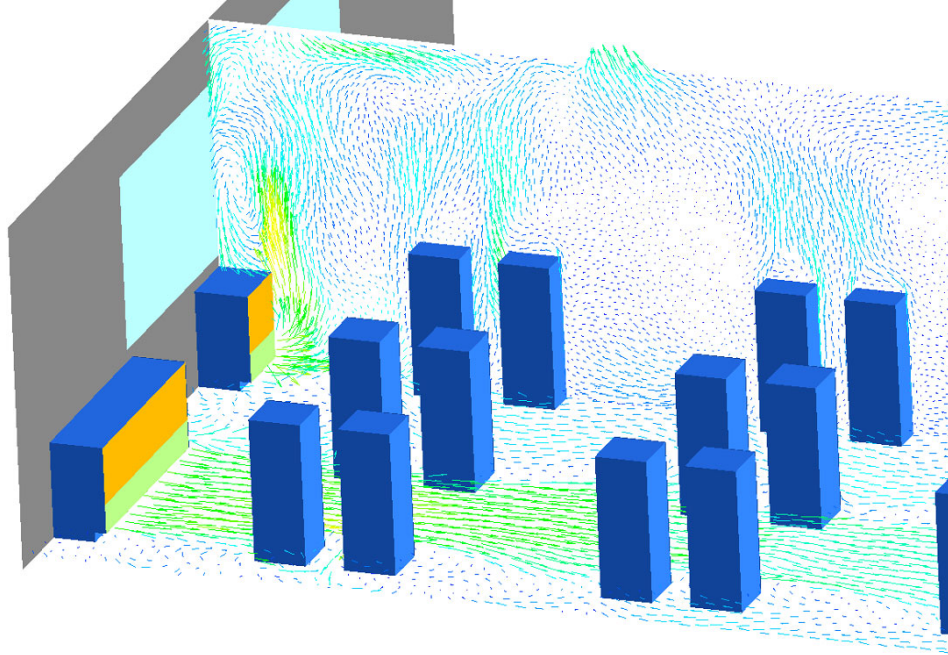
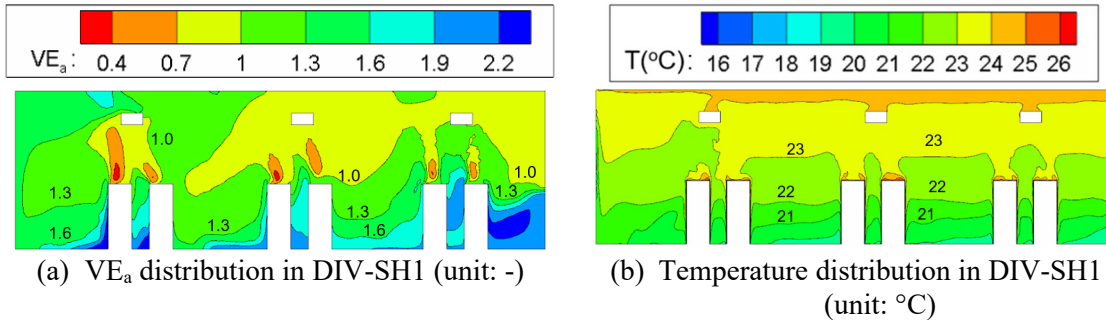


Fig. 10 Airflow distributions of two cross-sections in DIV-SH1 case

Similar as Fig. 9, Fig. 11 illustrates the air quality and temperature distributions on vertical planes when DIV system is used for heating. Because of the indoor airflow pattern described above, “staged-face heating” options generate stratified air distributions in the indoor space, as showed in Fig. 11 (a) and Fig. 11 (c). The quantitative comparison (Fig. 11g) further showed that DIV-SH1 presented slightly higher ventilation effectiveness than that in DIV-SH2. Figs. 11(b) and 11(d) illustrated the temperature stratification in the two cases, and the temperature gradients in occupied zone in both cases were within ASHRAE-55 requirement ($< 3\text{ }^{\circ}\text{C}$). Fig. 11 also reported the results in full-face heating mode (DIV-FH), a mode of operation traditionally reserved for low occupancy times such as morning warm up when increased heat input may be needed while ventilation effectiveness is less critical. The heating operation in DIV-FH continued to exude a stratified room condition and deliver a ventilation effectiveness greater than unity. By comparison with scenarios where warm air is delivered from traditional overhead diffusers or TDV diffusers, where VE_a can be as low as 0.8 to 0.7, the DIV-FH method showed better performance. It is important to note for these types of systems, when occupants are present, the occupant sensible heat load is considerable and very limited heat is required from the DIV units. The goal of the staged face heating strategy is to 1) more closely load match the room loads for optimal thermal comfort, 2) optimize ventilation effectiveness during heating, and 3) minimize utility consumption.



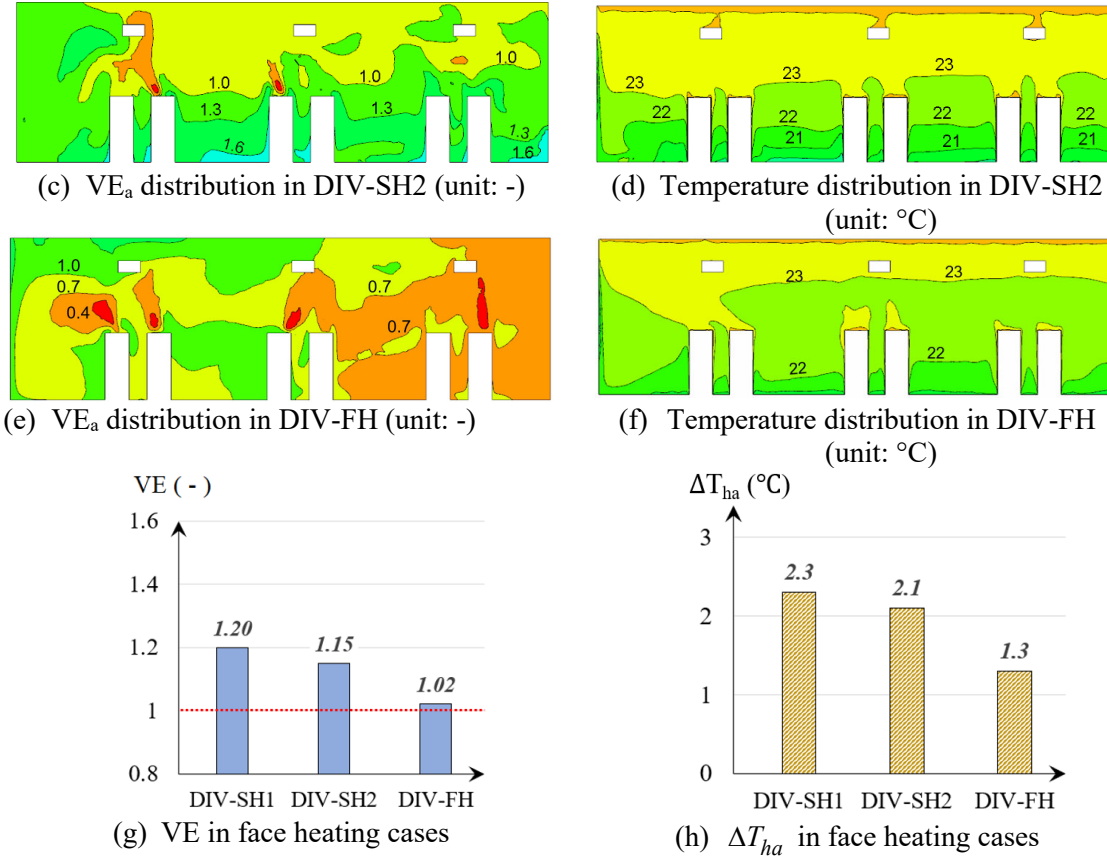


Fig. 11 Comparison of indoor environments created by face heating options

3.4 Performance of optional rear heating mode

This study further investigated the ventilation and thermal performance of DIV system in DIV-RH case. As demonstrated in Fig. 1, the chamber beneath rear heating coil is not enclosed but allows for an open pathway for ambient air. Hence, when hot water is delivered through the finned tube radiant coil, it drew surrounding room air towards the finned tube coils, heated the air up and created an upward air curtain to overcome the downward airflow typically recognized by cool window surface in cold climate regions. Meanwhile, the “cool” ventilation air discharged from front of DIV units was supplied to occupied zone directly, which resulted in stratified contaminant and temperature distributions throughout the room. Again, “cool” ventilation air is with respect to the bulk room temperature but still elevated from ambient conditions to provide occupant thermal comfort. Figs. 12(a) and 12(b) illustrate the VE_a and temperature distributions in DIV-RH case. The results were compared with the VE_a and temperature distributions of a traditional DV-R case, where similar finned tube hot water radiators were placed under window in a traditional DV system. Although a single traditional DV system was not recommended for delivering heated air to the space due to dominant buoyant forces driving the conditioned air upward versus delivering the air to the occupants [8], combining it with finned tube radiators allowed the traditional DV system to provide cool air to the occupied zone and hence retained contaminant stratification. Similar as in DV-C case, a similar rate of recirculation air was used for the DV part in this DV-R case. Overall, the ventilation performance of DIV-RH exceeds traditional DV-R, especially in the seated regions of the room where better IAQ is critically important, similar to the case for DIV-C (VE_a 2.2 to 1.3) versus DV-C (VE_a 1.3 to 1.0). As illustrated in Figs. 11(e) and 11(f), the thermal performances in both cases were acceptable.

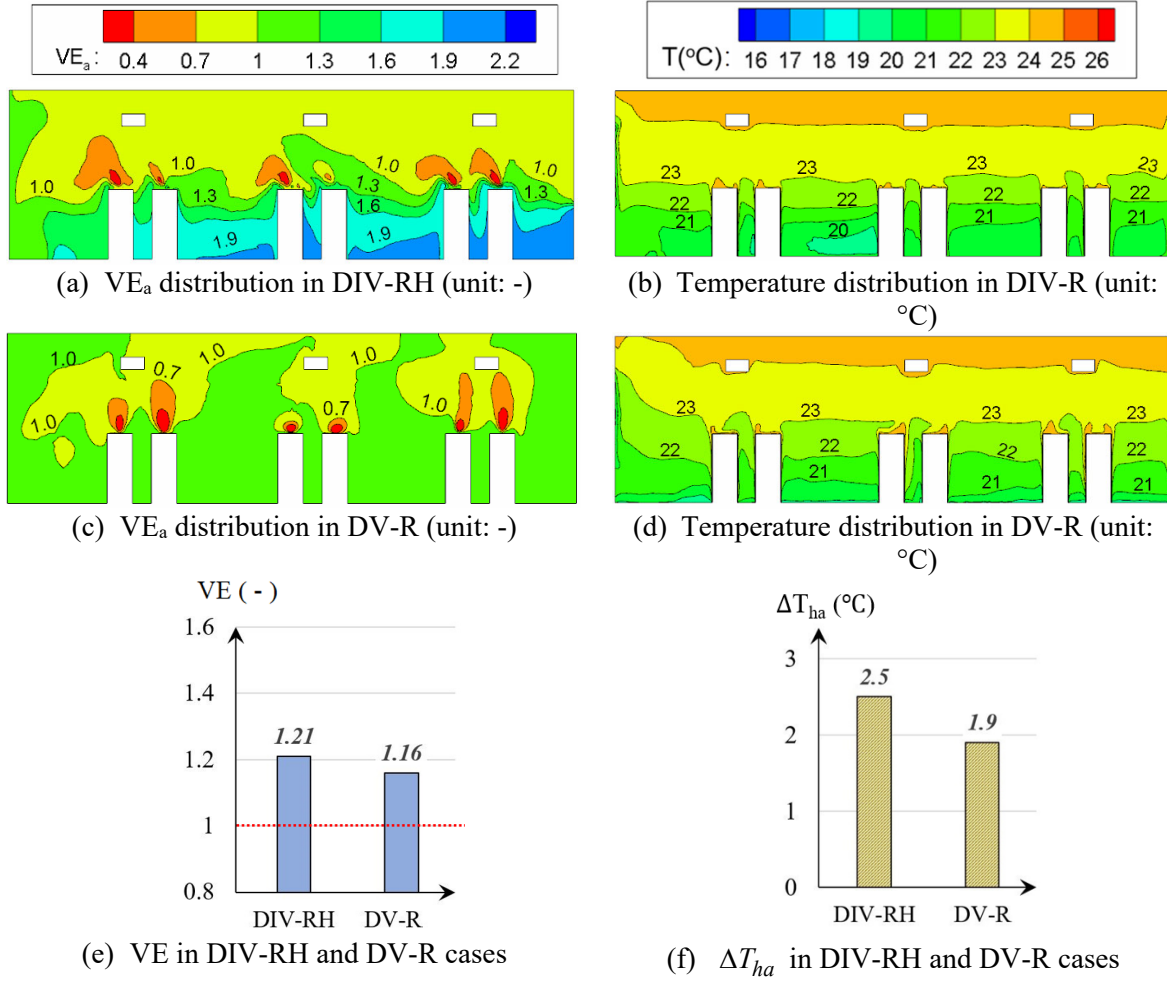


Fig. 12 Comparison of indoor environments created by DIV-RH and DV-R

381

382

3.5 MAA distributions in different operating modes

This study further investigated the MAA distributions of all the cases listed on Table 2. Fig. 13 demonstrates the MAA distributions in a cooling case (DIV-C), a face heating case (DIV-SH2) and a rear heating case (DIV-RH). In all the three cases, the MAA in occupied zone was lower than that in mixed zone, which again illustrated the capability of DIV system to create stratified air distribution under both cooling and heating modes. To quantitatively compare the MAAs of the air perceived by seated occupants in all the studied cases, Table 3 lists their average MAAs at breathing height (1.1 m above floor). As a reference, since the outdoor airflow rates in all these cases were equal, their MAAs at the exhaust were the same, and were equal to that in a perfectly designed mixed air system: 1311s (calculated via outdoor airflow rate and room volume). As noted in varying cases and shown in Fig. 13 below, the MAA at breathing height was at least 10% “fresher” than that at exhaust in DIV-C, DIV-SH1, DIV-SH2 and DIV-RH cases. These results presented a clear idea of the improved IAQ under various operating modes when the contaminant source locations were not specified, which again showed stratified conditions for DIV in both cooling and heating modes.

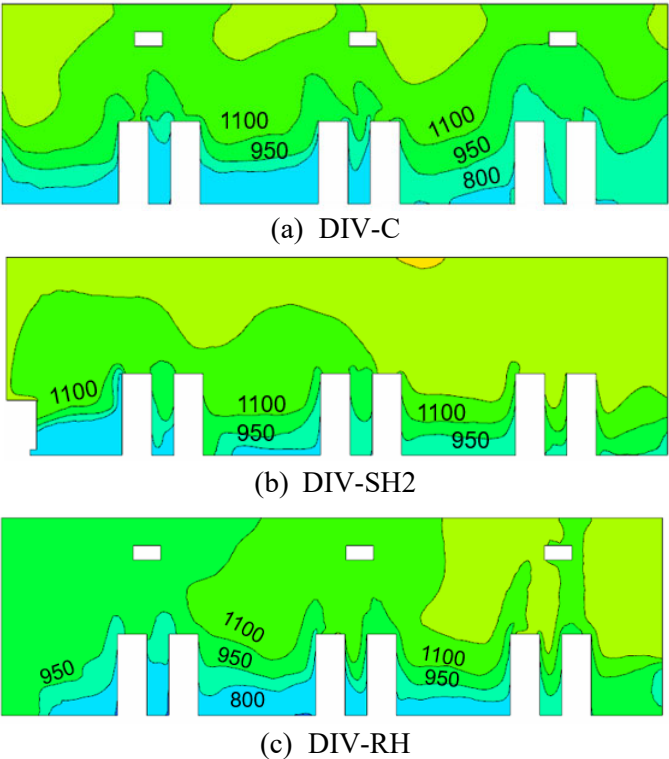


Fig. 13 MAA distributions in three representative cases (unit: s)

Table 3. Average MAA at breathing height for investigated cases (unit: s)

Case	DIV-C	DV-C	DIV-SH1	DIV-SH2	DIV-FH	DIV-RH	DV-R
------	-------	------	---------	---------	--------	--------	------

MAA	1079	1152	1113	1128	1291	1136	1193
-----	------	------	------	------	------	------	------

4. Discussions

4.1 Impact of DIV system layout on indoor environment

In this investigation, the three DIV units were installed at an equal distance between each other under the window. Although this was a reasonable layout, this was not the only option. An alternative was to place the three units adjacent to each other as a “compact layout”, which could leave some extra space at the corner of classroom for students. A hurdle for traditional DV systems which have one or two supply air diffusers is the aspect of near zone and uniform airflow and temperature distribution. The benefit of a full wall array DIV has potential benefits to deliver a more uniform airflow distribution and room environment. To mimic a compact or point source delivery of supply air, this study performed CFD simulations in cooling mode under a compact layout, and compared the results with those of original full-wall layout. A major concern for compact layout is it may lead to higher nonuniformity in temperature distribution, since the supply air is discharged from center of the classroom. Hence, particular attention was paid to the temperature uniformity, which could influence thermal comfort. Fig. 14 compares the temperature distributions at the ankle level (0.1 m) under the two layouts. With the same supply air temperature and flowrate, the average temperatures at the ankle level of the two layouts were the same. However, in compact layout, the temperature at the two corners of the classroom was 1 °C higher than that in the center, while in default layout the temperature distribution was a lot more uniform. The standard deviation (S.D.) of temperature at ankle level in compact layout was 16% higher than that in default layout. This comparison indicates the full-wall layout provided a better performance option in terms of thermal comfort.

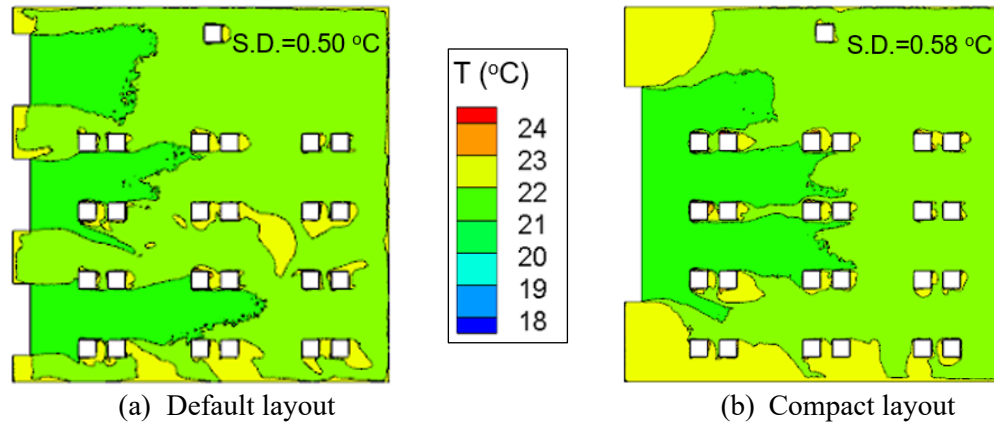


Fig. 14 Temperature distributions at ankle level in default layout and compact layout (unit: °C)

4.2 Droplet dispersion in indoor space with DIV system

In addition to gaseous contaminants, indoor contaminants could also be generated and transported in form of droplets, such as those originates from an occupant’s breathing, talking or coughing [46, 47, 48, 49]. With the same indoor space with human models, this investigation further studied the transport of particles with different diameters that were generated at an occupant’s head level. The particles could be of various diameters and particles’ behaviors could vary with particle size. Hence, this research selected four diameters to study their respective behaviors: 5 μm, 50 μm, 100 μm and 200 μm. The particles were released continuously for 5 seconds, and transient simulations were performed to study the dispersion of these particles over time.

435 To track the trajectories of the particles, Lagrangian method was adopted in the simulations. This
 436 method transiently solves the momentum equation that could be characterized as:

$$\frac{d\vec{u}_p}{dt} = F_D(\vec{u} - \vec{u}_p) + \frac{g(\rho_p - \rho)}{\rho_p} + \vec{F}_a \quad (6)$$

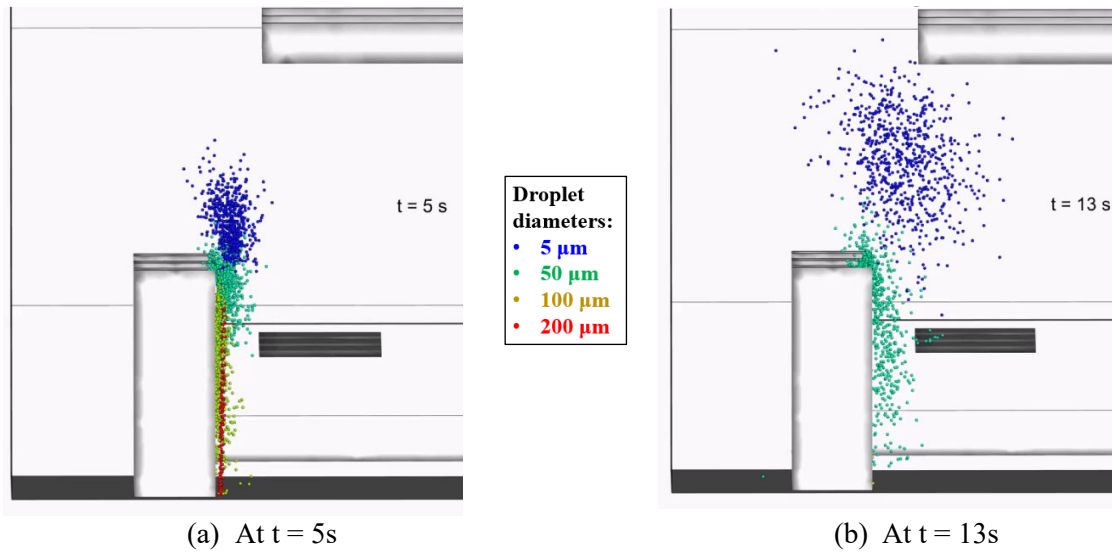
437 where \vec{u}_p , \vec{u} , ρ_p and ρ represent particle velocity vector, air velocity vector, particle density
 438 and air density, respectively. The left-hand side of Eq. (6) represents inertial force for a particle,
 439 while first term on right hand side represents drag term and second term on the right-hand side
 440 means gravitational force. Meanwhile, the discrete random walk (DRW) model was adopted to
 441 model the instantaneous velocity term u'_i , which correlates turbulent dispersion of particles with
 442 the flow turbulent kinetic energy as:

$$u'_i = \zeta \sqrt{2k/3} \quad (7)$$

443 where ζ is a random number, and k is turbulent kinetic energy. The number of particles released
 444 in the simulation was sufficient to capture the behaviors of these particles.

445 Fig. 15 demonstrates the distributions of particles at two time instances: 5 s (end of particle
 446 generation) and 13 s. It was observed that after the particles were released, the large particles (those
 447 with $d > 50 \mu\text{m}$) easily dropped onto the table or the floor. For these large particles, the gravitational
 448 force dominates their movements, so their dispersions are almost not affected by ventilation
 449 systems. On the other hand, the small particles, such as those with $d = 5 \mu\text{m}$, followed the indoor
 450 airflow after they were released. Because of thermal plume created by the occupant, these particles
 451 first moved up, similar as gaseous contaminants, and their movements afterwards greatly depended
 452 on the airflow distribution created in the room. The behaviors of these particles could hence be well
 453 described by the transport of gaseous contaminants. In fact, the conclusion that the dispersions of
 454 small particles and gaseous contaminants are similar were also reached in many previous studies,
 455 such as Mazumdar et al. [50] and Yin et al. [51]. Therefore, the results presented in section 3 not
 456 only quantified the effectiveness of DIV system in removing gaseous contaminants, but also
 457 quantified its overall effectiveness in removing droplets generated by occupants.

458



459 Fig.15 Dispersion of droplets with different diameters (droplets released from $t=0\text{s}$ to $t=5\text{s}$)

5. Conclusions

This investigation employed experimental and computational methods to explore the ventilation and thermal performance of a novel DIV system, per ASHRAE standards 62.1-2019 and 55-2017. It led to the following conclusions:

- (1) This study set up a DIV system which consisted of three DIV units in an IAQ chamber. Experimental measurements were performed to obtain the airflow velocity, air temperature and contaminant concentration distributions. Meanwhile, a CFD model was used to simulate the airflow and contaminant distribution in a room with DIV system. The results simulated by CFD matched within acceptable ranges with those obtained in lab validated experiment.
- (2) When used for cooling, DIV system created stratified air distribution. The ventilation effectiveness was shown to outperform that of a corresponding traditional DV system with the same percentage of return air. The resulting temperature gradient from ankle height to head height in occupied zone met the ASHRAE 55-2017 requirement.
- (3) When used for heating mode, utilizing the benefits of the outlined control strategy and unique equipment operation, the DIV system in staged heating modes DIV-SH1 and DIV-SH2 produced stratified contaminant distribution. DIV-SH1 yielded higher ventilation effectiveness as compared to DIV-SH2. The ventilation performance in full-face heating mode, traditionally used for low occupancy modes, was greater than unity and out-performed a traditional mixed air distribution delivering warm air. In addition, the ventilation effectiveness for the alternative “rear heating” mode also produced stratified room conditions, proving multiple heating strategies for delivering effective displacement ventilation. DIV-RH showed VE exceeds that of a combined traditional DV and radiator system.
- (4) In indoor spaces, particles with small diameters exhibit similar distribution as gaseous contaminants. Hence, the stratified air conditions resulting in a high level of ventilation effectiveness of DIV system demonstrated in this study could be also used to describe its increased effectiveness in removing particles generated in indoor environments.

Acknowledgement

The authors would like to thank Carson Solutions for sponsoring the research.

References

- [1] U.S. Environmental Protection Agency. (2019). Retrieved November 2019 from: <https://www.epa.gov/indoor-air-quality-iaq/inside-story-guide-indoor-air-quality#why-booklet>
- [2] Guieysse, B., Hort, C., Platel, V., Munoz, R., Ondarts, M., & Revah, S. (2008). Biological treatment of indoor air for VOC removal: Potential and challenges. *Biotechnology advances*, 26(5), 398-410.
- [3] Yu, J., Kang, Y., & Zhai, Z. J. (2020). Advances in research for underground buildings: Energy, thermal comfort and indoor air quality. *Energy and Buildings*, 215, 109916.
- [4] Wachenfeldt, B. J., Mysen, M., & Schild, P. G. (2007). Air flow rates and energy saving potential in schools with demand-controlled displacement ventilation. *Energy and buildings*, 39(10), 1073-1079.
- [5] Gilani, S., Montazeri, H., & Blocken, B. (2016). CFD simulation of stratified indoor environment in displacement ventilation: Validation and sensitivity analysis. *Building and Environment*, 95, 299-313.
- [6] Chen, C., Lai, D., & Chen, Q. (2020). Energy analysis of three ventilation systems for a large machining plant. *Energy and Buildings*, 224, 110272.

- [7] Chen, Q., Glicksman, L., Yuan, X., Hu, S., Hu, Y., & Yang, X. (1999). Performance Evaluation and Development of Design Guidelines for Displacement Ventilation—Final Report on ASHRAE Research Project RP-949.
- [8] Karimippanah, T., & Awbi, H. B. (2002). Theoretical and experimental investigation of impinging jet ventilation and comparison with wall displacement ventilation. *Building and Environment*, 37(12), 1329-1342.
- [9] Lau, J., & Chen, Q. (2006). Energy analysis for workshops with floor-supply displacement ventilation under the US climates. *Energy and Buildings*, 38(10), 1212-1219.
- [10] Price Industries. (2018). Displacement Ventilation Engineering Guide. Retrieved June 2019 from: <https://www.priceindustries.com/content/uploads/assets/literature/engineering-guides/displacement-ventilation-engineering-guide.pdf>
- [11] Cho, Y., Awbi, H. B., & Karimippanah, T. (2005). Comparison between wall confluent jets and displacement ventilation in aspect of the spreading ratio on the floor. In *Proceedings of the 10th International Conference in Indoor Air Quality and Climate*, Beijing, China (pp. 4-9).
- [12] Yuan, X., Chen, Q., & Glicksman, L. R. (1998). A critical review of displacement ventilation. *ASHRAE Transactions-American Society of Heating Refrigerating Airconditioning Engineers*, 104(1), 78-90.
- [13] Rees, S. J., & Haves, P. (2013). An experimental study of air flow and temperature distribution in a room with displacement ventilation and a chilled ceiling. *Building and Environment*, 59, 358-368.
- [14] Loveday, D. L., Parsons, K. C., Taki, A. H., & Hodder, S. G. (1998). Designing for thermal comfort in combined chilled ceiling/displacement ventilation environments/discussion. *ASHRAE transactions*, 104, 901.
- [15] Shi, Z., Lai, D., & Chen, Q. (2020). Performance evaluation and design guide for a coupled displacement-ventilation and passive-chilled-beam system. *Energy and Buildings*, 208, 109654.
- [16] Schiavon, S., Bauman, F., Tully, B., & Rimmer, J. (2012). Room air stratification in combined chilled ceiling and displacement ventilation systems. *HVAC&R Research*, 18(1-2), 147-159.
- [17] Shan, W., & Rim, D. (2018). Thermal and ventilation performance of combined passive chilled beam and displacement ventilation systems. *Energy and Buildings*, 158, 466-475.
- [18] ASHRAE, Standard 62.1-2019 Ventilation for Acceptable Indoor Air Quality. *American Society of Heating, Refrigerating and Air-Conditioning Engineers, Inc.*, Atlanta, GA, 40.
- [19] Cho, J., Lim, T., & Kim, B. S. (2009). Measurements and predictions of the air distribution systems in high compute density (Internet) data centers. *Energy and Buildings*, 41(10), 1107-1115.
- [20] Lin, Z., Tian, L., Yao, T., Wang, Q., & Chow, T. T. (2011b). Experimental and numerical study of room airflow under stratum ventilation. *Building and Environment*, 46(1), 235-244.
- [21] Calautit, J. K., & Hughes, B. R. (2014). Measurement and prediction of the indoor airflow in a room ventilated with a commercial wind tower. *Energy and Buildings*, 84, 367-377.
- [22] Bulińska, A., Popiołek, Z., & Buliński, Z. (2014). Experimentally validated CFD analysis on sampling region determination of average indoor carbon dioxide concentration in occupied space. *Building and Environment*, 72, 319-331.
- [23] Gan, G., & Awbi, H. B. (1994). Numerical simulation of the indoor environment. *Building and Environment*, 29(4), 449-459.
- [24] Yang, L., & Ye, M. (2014). CFD simulation research on residential indoor air quality. *Science of the Total Environment*, 472, 1137-1144.
- [25] Lee, S. C., & Wang, B. (2006). Characteristics of emissions of air pollutants from mosquito coils and candles burning in a large environmental chamber. *Atmospheric Environment*, 40(12), 2128-2138.

- [26] Norton, T., Grant, J., Fallon, R., & Sun, D. W. (2010). Optimising the ventilation configuration of naturally ventilated livestock buildings for improved indoor environmental homogeneity. *Building and Environment*, 45(4), 983-995.
- [27] Chen, Q., & Srebric, J. (2002). A procedure for verification, validation, and reporting of indoor environment CFD analyses. *HVAC&R Research*, 8(2), 201-216.
- [28] LumaSense Technologies. (2017). INNOVA 1312 User Manual. Retrieved from <https://innova.lumasenseinc.com/manuals/historical-manuals/1312/>
- [29] Pope, S. B. (2000). *Turbulent Flows*. Cambridge: Cambridge university press.
- [30] Yakhot, V., & Orszag, S. A. (1986). Renormalization group analysis of turbulence. I. Basic theory. *Journal of scientific computing*, 1(1), 3-51.
- [31] Yakhot, V. S. A. S. T. B. C. G., Orszag, S. A., Thangam, S., Gatski, T. B., & Speziale, C. G. (1992). Development of turbulence models for shear flows by a double expansion technique. *Physics of Fluids A: Fluid Dynamics*, 4(7), 1510-1520.
- [32] Zhang, Z., Zhang, W., Zhai, Z. J., & Chen, Q. Y. (2007). Evaluation of various turbulence models in predicting airflow and turbulence in enclosed environments by CFD: Part 2—Comparison with experimental data from literature. *Hvac&R Research*, 13(6), 871-886.
- [33] Gray, D. D., & Giorgini, A. (1976). The validity of the Boussinesq approximation for liquids and gases. *International Journal of Heat and Mass Transfer*, 19(5), 545-551.
- [34] Yuce, B. E., & Pulat, E. (2018). Forced, natural and mixed convection benchmark studies for indoor thermal environments. *International Communications in Heat and Mass Transfer*, 92, 1-14.
- [35] ANSYS Inc. (2016). *ANSYS Fluent Theory Guide 17.1*. Canonsburg, PA.
- [36] National Center for Education Statistics (NCES). 2011. Highest degree earned, years of full time teaching experience, and average class size for teachers in public elementary and secondary schools, by state: 2011-12. Retrieved July 2019 from: https://nces.ed.gov/programs/digest/d14/tables/dt14_209.30.asp?current=yes
- [37] Lau, J., & Chen, Q. (2007). Floor-supply displacement ventilation for workshops. *Building and Environment*, 42(4), 1718-1730.
- [38] Jin, M., Memarzadeh, F., Lee, K., & Chen, Q. (2012). Experimental study of ventilation performance in laboratories with chemical spills. *Building and environment*, 57, 327-335.
- [39] Li, X., Li, D., Yang, X., & Yang, J. (2003). Total air age: An extension of the air age concept. *Building and Environment*, 38(11), 1263-1269.
- [40] Aziz, M. A., Gad, I. A., El Shahat, F. A., & Mohammed, R. H. (2012). Experimental and numerical study of influence of air ceiling diffusers on room air flow characteristics. *Energy and Buildings*, 55, 738-746.
- [41] Jurelionis, A., Gagytė, L., Prasauskas, T., Čiužas, D., Krugly, E., Šeduikytė, L., & Martuzevičius, D. (2015). The impact of the air distribution method in ventilated rooms on the aerosol particle dispersion and removal: The experimental approach. *Energy and Buildings*, 86, 305-313.
- [42] Ilmarinen, R., Palonen, J., & Seppänen, O. (1992). Effects of non-uniform thermal conditions on body temperature responses in women. *Proceedings of the 41st Nordiska Arbetsmiljömötet*, 181-182.
- [43] Olesen, B. W., Scholer, M., & Fanger, P. O. (1979). Discomfort caused by vertical air temperature differences. *Indoor Climate*, 36, 561-578.
- [44] ASHRAE, A., & Standard, A. S. H. R. A. E. (2017). 55 2017. *Thermal Environmental Conditions for Human Occupancy*, American Society of Heating, Ventilating and Air-conditioning Engineers, Atlanta.
- [45] Chen, C., Zhu, J., Qu, Z., Lin, C. H., Jiang, Z., & Chen, Q. (2014). Systematic study of person-to-person contaminant transport in mechanically ventilated spaces (RP-1458). *HVAC&R Research*, 20(1), 80-91.

- [46] Gupta, J. K., Lin, C. H., & Chen, Q. (2010). Characterizing exhaled airflow from breathing and talking. *Indoor Air*, 20(1), 31-39.
- [47] Tham, K. W. (2016). Indoor air quality and its effects on humans—A review of challenges and developments in the last 30 years. *Energy and Buildings*, 130, 637-650.
- [48] Chen, L., Jin, X., Yang, L., Du, X., & Yang, Y. (2017). Particle transport characteristics in indoor environment with an air cleaner: The effect of nonuniform particle distributions. In *Building simulation* (Vol. 10, No. 1, pp. 123-133). Tsinghua University Press.
- [49] Berlanga, F. A., Olmedo, I., de Adana, M. R., Villafruela, J. M., San José, J. F., & Castro, F. (2018). Experimental assessment of different mixing air ventilation systems on ventilation performance and exposure to exhaled contaminants in hospital rooms. *Energy and Buildings*, 177, 207-219.
- [50] Mazumdar, S., Yin, Y., Guity, A., Marmion, P., Gulick, B., & Chen, Q. (2010). Impact of moving objects on contaminant concentration distributions in an inpatient ward with displacement ventilation. *Hvac&R Research*, 16(5), 545-563.
- [51] Yin, Y., Xu, W., Gupta, J. K., Guity, A., Marmion, P., Manning, A., ... & Chen, Q. (2009). Experimental study on displacement and mixing ventilation systems for a patient ward. *HVAC&R Research*, 15(6), 1175-1191.